Lifetime degradation and regeneration in multicrystalline silicon under illumination at elevated temperature

Dennis Bredemeier,[1] Dominic Walter,[1] Sandra Herlufsen,[1]
and Jan Schmidt[1,2]
[1]*Institute for Solar Energy Research Hamelin (ISFH), Am Ohrberg 1, 31860 Emmerthal, Germany*
[2]*Department of Solar Energy, Institute of Solid-State Physics, Leibniz University Hanover, Appelstr. 2, 30167 Hanover, Germany*

(Received 2 February 2016; accepted 13 March 2016; published online 22 March 2016)

We examine the carrier lifetime evolution of block-cast multicrystalline silicon (mc-Si) wafers under illumination (100 mW/cm^2) at elevated temperature (75°C). Samples are treated with different process steps typically applied in industrial solar cell production. We observe a pronounced degradation in lifetime after rapid thermal annealing (RTA) at 900°C. However, we detect only a weak lifetime instability in mc-Si wafers which are RTA-treated at 650°C. After completion of the degradation, the lifetime is observed to recover and finally reaches carrier lifetimes comparable to the initial state. To explain the observed lifetime evolution, we suggest a defect model, where metal precipitates in the mc-Si bulk dissolve during the RTA treatment. [http://dx.doi.org/10.1063/1.4944839]

Solar cells fabricated on multicrystalline silicon (mc-Si) wafers show a pronounced degradation in efficiency under illumination at temperatures higher than ~50°C.[1] Ramspeck *et al.*[1] showed that mc-Si solar cells with Al_2O_3/SiN_x-passivated rear surface lose up to 6% relative in their efficiency at an illumination intensity of 40 mW/cm^2 (0.4 suns) at 75°C on a timescale of about 400 hours, which he was not able to explain by known light-induced degradation processes such as the boron-oxygen defect activation[2–4] or the iron-boron pair dissociation.[5,6] The degradation was observed to a lesser extent on solar cells with a full-area aluminum back surface field (Al-BSF). Similar results were more recently reported by Fertig et al.,[7,8] who described the degradation of mc-Si passivated emitter and rear cells (PERC) on even larger timescales at 0.15 suns and 70°C. Most recently, Kersten et al.[9] observed the degradation effect on both passivated mc-Si lifetime samples as well as PERC solar cells. Interestingly, they also observed a full regeneration in the cell efficiency after approximately 150 hours of illumination at 0.3 suns and 95°C.

To improve the fundamental understanding of the degradation and regeneration processes, we conduct here experiments on mc-Si lifetime samples and implement industrial-type processing steps. We pay particular attention to the impact of rapid thermal annealing (RTA) steps, as typically applied in today's solar cell production lines as final and hence crucial thermal step. We implement two process flows, each with a variation in the RTA peak temperature. Both process flows are designed to represent a typical industrial-type PERC front- and rear-side process and are named process A (front) and process B (rear), respectively. We use block-cast boron-doped mc-Si wafers with a resistivity of 1.2 Ωcm and a size of 15.6 x 15.6 cm^2. The mc-Si material was grown in a G1 lab-size crucible[10] and contains the typical broad variety of metallic impurities, as examined by inductively-coupled plasma mass spectrometry (ICP-MS). Table I lists metallic impurities which were detected in total concentrations exceeding 10^{12} cm^{-3} in the as-grown material. Note that the mc-Si wafers used throughout this study are all neigbouring wafers stemming from a height of 34 to 43 mm above the brick's bottom.

The as-cut mc-Si wafers are first cleaned with a surface-active agent and subsequently etched in a potassium hydroxide solution to remove the saw damage. A phosphorus diffusion is then

TABLE I. List of metallic impurities, which were detected in total concentrations exceeding 10^{12} cm^{-3}, as examined by inductively-coupled plasma mass spectrometry (ICP-MS).

Metallic impurity	Concentration in cm^{-3}
Aluminum	3.72×10^{15}
Zirconium	8.19×10^{14}
Silver	3.97×10^{14}
Titanium	3.26×10^{14}
Iron	2.02×10^{14}
Tungsten	1.58×10^{14}
Copper	8.30×10^{13}
Yttrium	7.72×10^{13}
Nickel	4.26×10^{13}
Chromium	1.17×10^{13}
Vanadium	7.26×10^{12}
Molybdenum	6.45×10^{12}
Cobalt	5.27×10^{12}
Manganese	3.07×10^{12}

performed in a quartz-tube furnace at a process temperature of 853°C resulting in n^+-layers on both wafer surfaces with a sheet resistance between 50 and 60 Ω/sq. After the phosphorus diffusion, the wafers are divided into two groups. Within group A, a SiN_x layer of 100 nm and a refractive index of 2.05 is deposited on top of each n^+-layer using an industrial-type plasma-enhanced chemical vapor deposition (PECVD) process (Roth&Rau, SiNA). The n^+-layers of group B are chemically removed by a solution of hydrofluoric acid and nitric acid using a chemical polishing process. The surfaces are then passivated by an Al_2O_3/SiN_x-stack, where the Al_2O_3 layer is deposited by spatial atomic layer deposition (ALD) in an InPassion LAB System (SolayTec) with a thickness of 5nm. The SiN_x layers are deposited with the same process as stated for group A. Both groups of wafers receive as a final step an RTA firing treatment at two different set peak temperatures using an industrial conveyor belt furnace (centrotherm photovoltaics, DO-FF-8.600-300). Two of the samples within each group are fired at a set peak temperature of 900°C and the other one at 650°C. The belt speed is set at 6.8 m/min. Those peak temperatures are chosen to cover the range of relevant temperatures in a typical solar cell fabrication process and to clearly separate the impact of different firing conditions on the light-induced degradation and regeneration processes. All wafers are stored in the dark at room temperature to prevent any degradation prior to the actual experiments.

Injection-dependent carrier lifetimes are measured using the photoconductance decay (PCD) and the quasi-steady-state photoconductance (QSSPC) techniques[11] within a circular area with a diameter of 18 mm located in the upper right corner of the wafers (orientations as in Figs. 4 and 5). Spatially resolved lifetime measurements are carried out using the photoconductance-calibrated photoluminescence imaging (PC-PLI) method.[12] The samples are illuminated with halogen lamps at 1 sun light intensity at 75°C. The effective carrier lifetimes are measured at defined timesteps. The mc-Si lifetime samples of both groups fired at a set peak temperature of 900°C show a pronounced degradation in the lifetime, as can be seen in the lifetime measurements shown in Figs. 1 and 2, which represent the typical behaviour of the respective sample types. The observed lifetime degradation can be subdivided into two stages. The first stage is finalised within the first 2 hours and is characterized by a fast and pronounced reduction in lifetime. This stage is followed by a slower exponential degradation, terminating within ~100 hours. Fitting an exponential decay to the slow degradation results in time constants of 22.7 hours for samples of group A and 55.6 hours for samples of group B. We verified the presence of at least two stages of degradation – a fast and a slow one – by additional measurements on mc-Si wafers of a different ingot, which were identically processed (see Fig. 3 and corresponding discussion below). Note that the presence of two stages of degradation was also observed on mc-Si solar cells in the study by Ramspeck et al.,[1] where the published degradation data cannot be fitted with a single-exponential decay, but require a fast

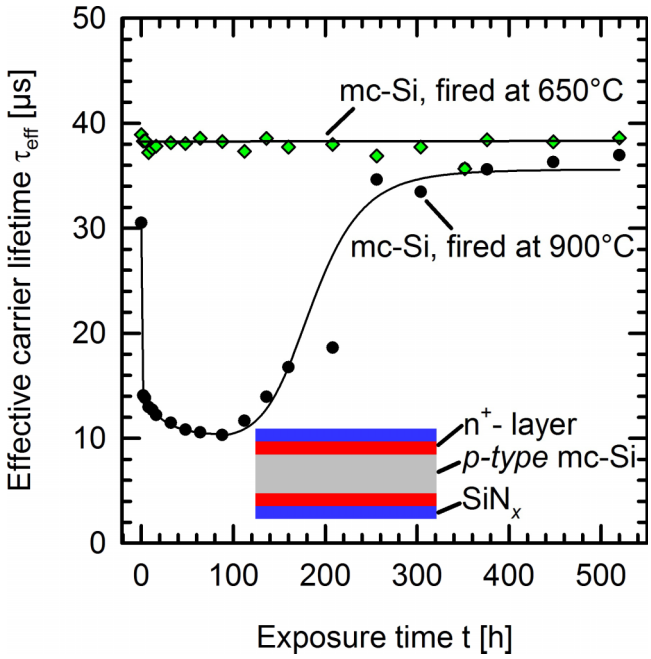

FIG. 1. Effective carrier lifetime measured at $\Delta n = 10^{15}$ cm^{-3} by the QSSPC technique of mc-Si lifetime samples from group A plotted versus the exposure time of illumination at 1 sun at 75°C. The solid lines are guides to the eyes.

initial plus a slow degradation component. After complete degradation, Figs. 1 and 2 show that the lifetimes increase again ('regeneration') and finally reach values even higher than the initial lifetime. Note that we cannot exclude that the initial lifetime measurement has been performed in a slightly degraded state. If this has been the case, the regeneration would not reach necessarily higher lifetimes than the initial ones, but just comparable lifetimes to the initial state. One of the most

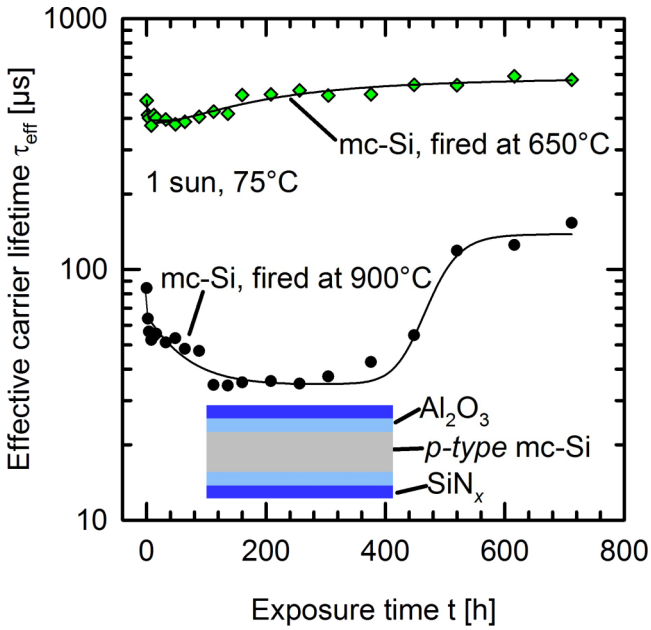

FIG. 2. Effective carrier lifetime measured at $\Delta n = 10^{15}$ cm^{-3} by the PCD (diamonds) and the QSSPC (circles) techniques of mc-Si lifetime samples from group B plotted versus the exposure time of illumination at 1 sun at 75°C. The solid lines are guides to the eyes.

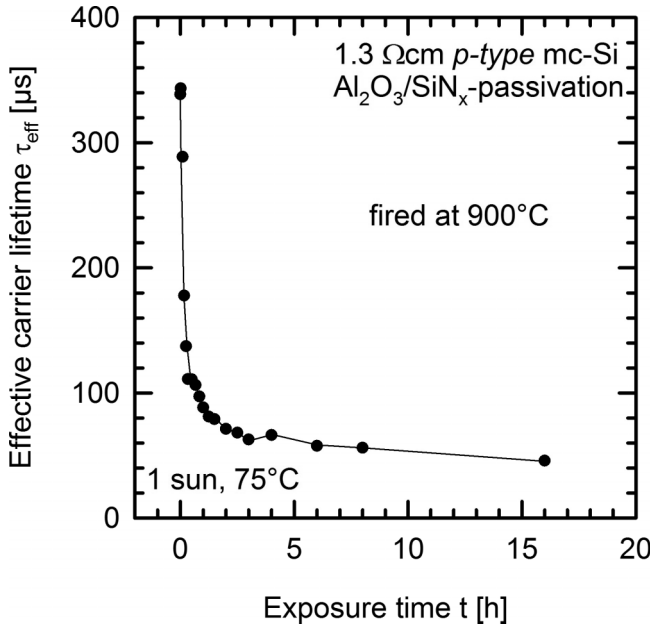

FIG. 3. Effective carrier lifetime of a mc-Si lifetime sample which underwent process B, measured by the QSSPC technique at $\Delta n = 10^{15}$ cm^{-3} and plotted versus the exposure time of illumination at 1 sun at 75°C.

important findings of this study is our observation that the samples fired at a reduced peak temperature of 650°C remain stable for group A and show only a very weak degradation from 472 µs to 375 µs in the case of group B, as can be seen in Figs. 1 and 2. Note that even if the temperature of 853°C during phosphorus diffusion might dissolve some of the metal precipitates present in our material, the very slow cooling process after diffusion will most likely lead to a re-formation of a large fraction of the precipitates. As the cooling ramp after the RTA process is orders of magnitude higher, there is not enough time after the RTA step to re-form the precipitates.

Figure 3 shows the lifetime evolution of a mc-Si lifetime sample which underwent process B, recorded with a higher time resolution compared to Figs. 1 and 2. The sample was processed from a different block-cast boron-doped mc-Si ingot grown under comparable conditions as the ingot examined in Figs. 1 and 2. It is obvious from Fig. 3 that the lifetime evolution cannot be described by a single-exponential decay function. However, the fast component of degradation is clearly visible to be terminated after less than 1 hour.

Figures 4 and 5 show PC-PLI lifetime measurements of the degradation and regeneration for the samples fired at 900°C set peak temperature as shown in Figs. 1 and 2, respectively. The excitation level is chosen to result in an area-averaged excess carrier concentration of 10^{14} cm^{-3}. For group A as well as group B, the fast and slow degradations occur relatively homogeneous over the wafer area. Please note that the edge regions show a reduced lifetime even in the initial lifetime images due to impurities diffusing from the crucible into the bulk material during the crystallization process. The degradation can be clearly observed when comparing the lifetime images shown in Figs. 4(a) and 4(b). While Fig. 4(a) shows the initial lifetime of the wafer, image (b) is taken after 48 hours of light exposure at 1 sun and 75°C. To further quantify the homogeneity of the degradation, we investigate the time constants at 100 non-overlapping 1×1 cm^2 squares over the wafer area. We determine a time constant for the wafer shown in Fig. 5 (group A) of 20 ± 5 hours and for the wafer shown in Fig. 4 (group B) of 60 ± 14 hours. The moderate variations in the degradation time constants over the wafer area demonstrate that the degradation is proceeding quite homogeneously over the wafer area. Note that on a microscopic scale there might exist some superimposed lifetime degradation inhomogeneities, which are, however, not in the focus of this study as they are not the main degradation mechanism in large-area mc-Si solar cells.

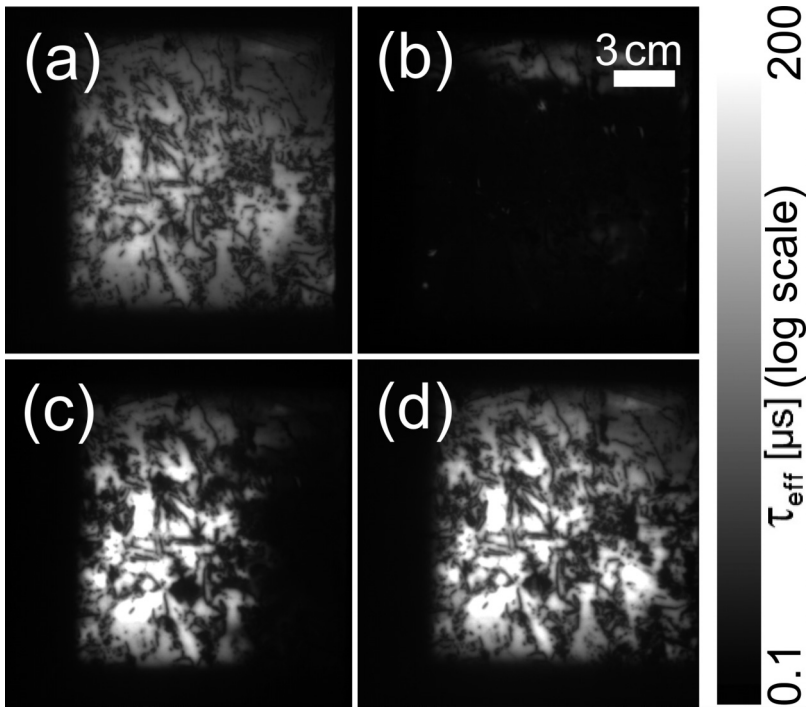

FIG. 4. Lifetime images measured by PC-PLI of an mc-Si lifetime sample from group B at different timesteps during illumination at 1 sun light intensity and 75°C. (a) Initial state, (b) after 48 hours of illumination, (c) after 448 hours, (d) after 616 hours.

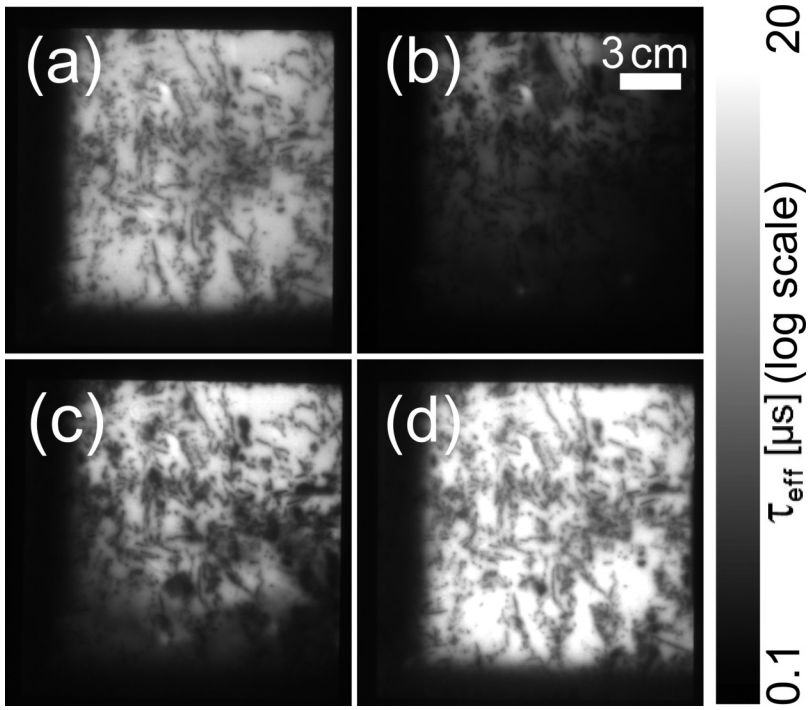

FIG. 5. Lifetime images measured by PC-PLI of an mc-Si lifetime sample from group A at different timesteps during illumination at 1 sun light intensity and 75°C. (a) Initial state, (b) after 208 hours, (c) after 256 hours, (d) after 520 hours.

In contrast to the lifetime degradation, the regeneration is a rather inhomogeneous process. As can be seen in Figs. 4 and 5, the regeneration starts locally and is then spreading out over the wafer area. In Fig. 5, the lifetime image (a) is followed by image (b) showing the very beginning of regeneration after 208 hours. During prolonged illumination at elevated temperature the inhomogeneity of the regeneration can be observed comparing the images (c) of Figs. 4 and 5, with the fully regenerated state in Figs. 4 and 5(d). The general structure of grain boundaries and dislocation clusters visible in the lifetime image does not change during degradation nor regeneration. Importantly, we observe that the regeneration time constants correlate with the wafer thicknesses, which feature a wedge profile. The wafer shown in Fig. 4 has a thickness of 198 μm at the left wafer edge and a thickness of 219 μm at the right edge, whereas the wafer shown in Fig. 5 has a thickness of 192 μm at the top wafer edge and a thickness of 203 μm at the bottom edge.

As a reference, monocrystalline Czochralski-silicon (Cz-Si) wafers were processed in parallel to the mc-Si wafers. On the boron-doped Cz-Si wafers with a resistivity of 4.5 Ωcm we observe the well-known degradation and regeneration processes associated with the boron-oxygen complex, which are, however, very different concerning the time constants compared to our observations on mc-Si. The lowest effective carrier lifetime measured on the Cz-Si reference wafers was 124 μs for group A and 671 μs for group B, thus well above the highest lifetimes of the corresponding mc-Si samples. Hence, we conclude that a degradation of the surface passivation quality of the samples cannot be considered the main cause of the observed behaviour.

The degradation on our mc-Si samples *cannot* be explained through the activation of the well-known boron-oxygen complex[13] nor by iron-boron pair dissociation.[14] On the one hand, the interstitial oxygen [O_i] concentration in the examined mc-Si material is only 1×10^{17}cm^{-3} as measured by fourier transform infrared spectroscopy (FTIR) compared to typical [O_i] concentrations in Cz-Si of $(7-8) \times 10^{17}$cm^{-3}. On the other hand, the boron-oxygen-related degradation is taking place on a different timescale with a fast component taking place within seconds and a slow component taking place with a time constant of 0.2 hours at 75°C on 1.2 Ωcm Cz-Si.[15] As also determined via FTIR, the substitutional carbon concentration [C_s] of the material examined in this study is 1x10^{17} cm^{-3} and the nitrogen dimer concentration [N_2] is 3x10^{15} cm^{-3}. Note that Ramspeck et al.[1] conducted additional experiments on gallium-doped mc-Si material. These wafers showed the same degradation behavior as the boron-doped wafers, excluding any boron-related degradation mechanism. We have excluded the possibility of iron-boron pair dissociation by storing our samples for two days in the dark and measuring the effective carrier lifetime in the center of the wafers in the presumably associated state of the iron-boron pair. These results have been compared to those retrieved from lifetime measurements after flashing the samples with high light intensity.[14] Because the dissociation of iron-boron pairs through flashing would have been visible by a change in the effective carrier lifetime,[14] the lack of that effect is a clear indication that our mc-Si samples do not show any iron-boron-related degradation.

In the following, we propose a (hypothetical) defect model which is consistent with our experimental observations. However, note that further experimental verifications are required to verify or falsify the various aspects of the proposed model. Let us assume that latent precipitates of a particular metal (M_P) are present in the as-grown mc-Si material, which is a realistic assumption as high concentrations of various metals have been detected in our material via ICP-MS (see above). Since we observe the degradation and regeneration cycle only after belt-firing at sufficiently high temperature (900°C), we assume that the precipitates M_P dissolve during the high-temperature RTA into mobile, most likely interstitial metal atoms M_i, whereas the precipitates M_P do not (or only partly) dissolve at the lower firing temperature of 650°C. As the metal precipitates (probably nano-precipitates) are present in a relatively small density, their impact on the bulk lifetime is weak. After dissolving into the interstitial metal atoms, during the rapid cooling after the peak temperature, the M_i are conjectured to be captured by another homogeneously distributed impurity X (e.g. O_i, C_s, N_2, H) to form an $M_i - X$ complex. The $M_i - X$ complex is assumed to be a relatively weak recombination center and is present only directly after the high-temperature RTA step. During illumination at elevated temperature, the $M_i - X$ complex might change its configuration into a more recombination-active form $M_i - X^*$, which subsequently dissociates into isolated M_i and X. While the reconfiguration of the $M_i - X$ complex is assumed to be responsible for the fast component

of the lifetime degradation, the isolated M_i is assumed to be highly recombination active, thus explaining the slow degradation of the bulk lifetime of our samples. During prolonged illumination at elevated temperature, the mobile M_i atoms diffuse to the wafer surfaces, where the M_i are trapped. Due to the inhomogeneous wafer thickness and therefore a spatially inhomogeneous period for the M_i to diffuse to the wafer surface, the lifetime regeneration is strongly position-dependent. The wafer surfaces are of course not the only possible sink for the fast diffuser M_i. Another category of sinks are the inhomogeneously distributed crystallographic defects in the mc-Si material, where the M_i might attach to. The proposed model – although admittedly still in a speculative phase – explains both the homogeneous lifetime degradation as well as the relatively inhomogeneous regeneration, which is primarily correlated with the wafer thickness and, secondary, with the distribution of crystallographic defects. Finally, it should be noted that hydrogen might play a certain role in the exact defect chemistry and might even be directly related to the defect X. It is well known that RTA treatment in combination with hydrogen-rich SiN_x layers deposited at the wafer surfaces leads to hydrogen injection into the mc-Si bulk.[16] Hence, in particular our wafers fired at 900°C are expected to contain some hydrogen.

In conclusion, we have shown that a high-temperature RTA treatment has a strong impact on the lifetime degradation and regeneration behaviour of mc-Si wafers under illumination at elevated temperature (100 mW/cm^2, 75°C). Samples treated during a fast-firing step with a set-peak temperature of 900°C showed a pronounced light-induced lifetime degradation and regeneration, whereas the lifetime of mc-Si samples treated with a maximum peak temperature of 650°C remained stable. In addition, we observed that the lifetime evolution under illumination at elevated temperature can be subdivided into three stages. At first, there is a fast and spatially relatively homogeneous degradation of the lifetime completed within the first two hours of illumination, followed by a slow and also homogeneous degradation in the second stage. The slow degradation terminates within a period of ~100 hours. The third stage is an inhomogeneous regeneration of the lifetime to values comparable to the initial state or even above. In order to explain the observed lifetime behavior, we have suggested a first speculative defect model, in which metal precipitates are assumed to dissolve in the high-temperature RTA treatment into interstitial impurities M_i and bind during the cooling after RTA to a homogeneously distributed defect X. The $M_i - X$ complex transforms under illumination at elevated temperature first into a more recombination-active form $M_i - X^*$ and then dissociates into a highly recombination-active M_i and a passive X, thus leading to a homogeneous lifetime degradation. During the subsequent regeneration, the M_i atoms diffuse to the surfaces or/and to inhomogeneously distributed crystallographic defects, explaining the observed inhomogeneity of the regeneration process, which is directly correlated with the wafer thickness (the thinner the wafer the faster is the regeneration). One might conjecture that hydrogenation could also play a role in the detailed defect physics. However, further experiments involving hydrogen-free surface passivation layers are required to verify the possible influence of hydrogen. From a practical point of view, our experimental results suggest an easy-to-implement approach to avoid degradation in industrially produced mc-Si solar cells by reducing the peak firing temperature below the critical temperature ϑ_c required to dissolve the latent metal precipitates. Based on our experimental findings, we can conclude that the critical temperature ϑ_c is in the range between 650°C and 900°C, however, more detailed investigations are necessary to pinpoint the exact value of ϑ_c.

The authors acknowledge S. Meyer from Fraunhofer CSP for the ICP-MS measurements and T. Arguirov from BTU Cottbus for the FTIR measurements. This work was funded by the German State of Lower Saxony and the German Federal Ministry of Economics and Energy and by industry partners within the research project "SolarLIFE" (contract no. 0325763C). The content is the responsibility of the authors. The publication of this article was funded by the Open Access fund of Leibniz Universität Hannover.

[1] K. Ramspeck, S. Zimmermann, H. Nagel, A. Metz, Y. Gassenbauer, B. Birkmann, and A. Seidl, in *Proceedings of the 27th European Photovoltaic Solar Energy Conference* (WIP, Munich, 2012), p. 861.

[2] J. Schmidt, A. G. Aberle, and R. Hezel, in *Proceedings of the 26th IEEE Photovoltaic Specialists Conference* (IEEE, New York, 1997), p. 13.

[3] S. W. Glunz, S. Rein, W. Warta, J. Knobloch, and W. Wettling, in *Proceedings of the 2nd World Conference on Photovoltaic Energy Conversion* (WIP, Munich, 1998), p. 1343.

[4] J. Schmidt and K. Bothe, Phys. Rev. B **69**, 024107 (2004).
[5] L. J. Geerligs and D. Macdonald, Appl. Phys. Lett. **85**, 5227 (2004).
[6] J. Schmidt, Prog. Photovolt. **13**, 325 (2005).
[7] F. Fertig, K. Krauß, and S. Rein, Phys. Status Solidi RRL **9**, 41 (2014).
[8] K. Krauss, F. Fertig, D. Menzel, and S. Rein, Energy Procedia **77**, 599 (2015).
[9] F. Kersten, P. Engelhart, H.-C. Ploigt, A. Stekolnikov, T. Lindner, F. Stenzel, M. Bartzsch, A. Szpeth, K. Petter, J. Heitmann, and J.W. Müller, Solar Energy Materials and Solar Cells **142**, 83 (2015).
[10] W. Kwapil, A. Zuschlag, I. Reis, I. Schwirtlich, S. Meyer, R. Zierer, R. Krain, F. Kießling, M. Schumann, C. Schmid, and S. Riepe, in *Proceedings of the 27th European Photovoltaic Solar Energy Conference* (WIP, Munich, 2012), p. 627.
[11] R. A. Sinton and A. Cuevas, Appl. Phys. Lett. **69**, 2510 (1996).
[12] S. Herlufsen, J. Schmidt, D. Hinken, K. Bothe, and R. Brendel, Phys. Stat. Sol. RRL **2**, 245 (2008).
[13] K. Bothe and J. Schmidt, J. Appl. Phys. **99**, 013701 (2006).
[14] R. Krain, S. Herlufsen, and J. Schmidt, Appl. Phys. Lett. **93**, 152108 (2008).
[15] D. Palmer, K. Bothe, and J. Schmidt, Phys. Rev. B **76**, 035210 (2007).
[16] F. Jiang, M. Stavola, A. Rohatgi, D. Kim, J. Holt, H. Altwater, and J. Kalejs, Appl. Phys. Lett. **83**, 931 (2003).